

# QCD Studies and Determination of $\alpha_s$ in $e^+e^-$ collisions at $\sqrt{s} = 161$ GeV and 172 GeV

L3 Collaboration

## Abstract

We present a study of the structure of hadronic events recorded by the L3 detector at LEP at the center of mass energies of 161 and 172 GeV. The data sample corresponds to an integrated luminosity of  $21.25 \text{ pb}^{-1}$  collected during the high energy runs of 1996. The distributions of event shape variables and the energy dependence of their mean values are well reproduced by QCD models. From a comparison of the data with resummed  $\mathcal{O}(\alpha_s^2)$  QCD calculations, we determine the strong coupling constant at the two energies. Combining with our earlier measurements we find that the strong coupling constant decreases with increasing energy as expected in QCD.

Submitted to *Phys. Lett. B*

# Introduction

The LEP machine has increased the beam energies above the  $W^+W^-$  pair production threshold during 1996. There have been two runs corresponding to center of mass energies of the  $e^+e^-$  system of 161 GeV and 172 GeV allowing us to test the predictions of the theory of the strong interaction (QCD) [1] by studying  $e^+e^- \rightarrow q\bar{q}$  at these new energies. Earlier tests have been done at 91 GeV with hadronic Z decays [2–5] and with  $e^+e^-$  interactions at center of mass energies between 130 and 136 GeV [6, 7].

We report on the studies of several event shape variables for these high energy hadronic final states. The distributions have been corrected for detector effects, background contamination from  $W^+W^-$  pair production and hard photon radiation. These distributions are then compared with QCD models which have been used extensively at  $\sqrt{s} = 91$  GeV and for which the parameters have been tuned using hadronic Z decays. The energy dependence of the mean value of several global event shape variables and charged particle multiplicity measured at different center of mass energies is in agreement with QCD models. We also measure the jet rates in these hadronic events.

The measured distributions of event shape variables are compared to the predictions of a second-order QCD calculation with resummed leading and next-to-leading terms. This provides a determination of the strong coupling constant  $\alpha_s$  at the two energies. We use our previous  $\alpha_s$  measurements at  $\sqrt{s} = 91$  GeV [3, 4] and 133 GeV [6] from a similar analysis to compare the relative change with the QCD expectation.

## Selection of Hadronic Events

For this analysis, we use data corresponding to integrated luminosities of 11.05  $\text{pb}^{-1}$  and 10.2  $\text{pb}^{-1}$  collected by the L3 detector [4, 8] during 1996 at center of mass energies ( $\sqrt{s}$ ) of 161 GeV and 172 GeV respectively.

The selection of  $e^+e^- \rightarrow$  hadrons events is based on the energy measured in the electromagnetic calorimeter composed of BGO crystals and in the uranium hadronic calorimeter with proportional wire chamber readout. We use energy clusters in the calorimeters with a minimum energy of 100 MeV. The number of clusters is denoted by  $N_{cluster}$ . We measure the total visible energy ( $E_{vis}$ ) and the energy imbalance parallel ( $E_{\parallel}$ ) and perpendicular ( $E_{\perp}$ ) to the beam direction. We classify an event as hadronic if the event satisfies the following cuts:

- $N_{cluster} \geq 13$
- $0.6 < E_{vis}/\sqrt{s} < 1.4$
- $E_{\perp}/E_{vis} < 0.4$ .
- $N_{track} > 1$

where  $N_{track}$  is the number of tracks measured in the central tracking chamber with a magnetic field of 0.5 T. The tracks are selected by requiring at least 30 hits on each of them and a transverse momentum greater than 100 MeV.

Monte Carlo hadronic events were generated by the parton shower program PYTHIA 5.7 [9] and passed through the L3 detector simulation [10]. 96% of the simulated hadronic events are accepted by these cuts.

A large fraction of the events are accompanied by a photon from hard initial state radiation (ISR). The mass recoiling against the photon is often close to that of the Z boson, due to the large Z-pole cross section. The fraction of events with hard initial state radiation in our sample is about 65%. To reduce this contamination, the following two cuts have been applied:

- $(E_{vis}/\sqrt{s}) > a(|E_{\parallel}|/E_{vis}) + 0.5$
- energy of the most energetic photon,  $E_{\gamma} < 30$  GeV.

where  $a=1.5$  at 161 GeV and  $a=2.0$  at 172 GeV. The first cut uses the correlation between  $E_{vis}/\sqrt{s}$  and  $|E_{\parallel}|/E_{vis}$ , which is shown in figure 1a for data at 161 GeV. It discriminates well balanced events from unbalanced events arising from an ISR photon lost in the beam pipe. However, the well balanced events could contain initial state radiation where the photon is seen in the detector. These are removed by the second cut when a neutral cluster compatible with a high energy photon of more than 30 GeV is found in the BGO calorimeter. Figure 1b shows the energy distribution of the most energetic photon detected in the BGO calorimeter at 161 GeV with a peak near 54 GeV corresponding to a recoil mass around  $m_Z$ .

The selected samples contain 443 hadronic events at 161 GeV and 386 at 172 GeV. Applying the above cuts to fully simulated events we find that 90% of hadronic events with no hard initial state radiation greater than 30 GeV are accepted.

The main sources of background are due to  $W^+W^-$  decays and two-photon collisions ( $e^+e^- \rightarrow e^+e^- + \text{hadrons}$ ). Applying the same cuts to background Monte Carlo events produced by the KORALW generator [11] for the  $W^+W^-$  events and by the PYTHIA generator [12] for the two-photon events, the contamination in the selected hadron sample at 161 GeV is estimated to be about 4% and 3% respectively. At 172 GeV the event sample contains about 17% of  $W^+W^-$  background and 3% of two-photon events.

The background contamination due to the  $W^+W^-$  final state is rather small at 161 GeV and hence we adopted a bin by bin background subtraction at this energy. However, the level of contamination of  $W^+W^-$  events is quite substantial at 172 GeV. Additional cuts are therefore used to reduce the level of this background. After removing the events with energetic muons (momentum greater than 40 GeV) the remaining events are forced to form four jets using the Durham algorithm [13]. The jet energies are then rescaled under the assumptions that the jet directions are exact and there is no missing energy. The jets are energy ordered and then the following cuts are used to classify the event in the  $W^+W^-$  category :

- $N_{cluster} \geq 40$  ;  $N_{track} > 15$
- $E_{jet1} < 0.4\sqrt{s}$  ;  $E_{jet4} > 0.1\sqrt{s}$
- $y_{34}^D \geq 0.007$

where  $y_{34}^D$  is the jet resolution parameter for which the event goes from four to three jet topology. Figure 2 shows the  $y_{34}^D$  distribution for the events passing the first four cuts. In general there is a good agreement in the shape between data and Monte Carlo predictions. The separation power of this variable is such that the cut at 0.007 selects 53% of the  $W^+W^-$  events contained in the selected non-radiative event sample with a purity of 78%.

After rejecting these identified events, the final sample at 172 GeV contains 341 events. The background contamination from  $W^+W^-$  events is about 9% and the efficiency to select hadronic events with no hard ISR with energy greater than 30 GeV is 85%. The data have been corrected for the effects of remaining ISR using the PYTHIA [9] Monte Carlo event generator.

Table 1 summarises the background content of the remaining event samples at 161 GeV and 172 GeV.  $Ze^+e^-$  and  $ZZ$  events amount to 1% of the overall sample while  $\tau$  pair final state events contribute a negligible background.

# Global Event Shape Variables

The jet structure of hadronic events can be analysed using global event shape variables. We limit our study to four variables - thrust ( $T$ ), scaled heavy jet mass ( $\rho$ ), total ( $B_T$ ) and wide ( $B_W$ ) jet broadenings, for which improved analytical QCD calculations are available [14–17]. We also measure the charged particle multiplicity distribution. We have previously measured these variables at  $\sqrt{s} = 91$  GeV [4, 18] and at 130 and 136 GeV [6].

The charged particle multiplicity distribution is obtained from reconstructed tracks while the other event shape distributions are obtained from reconstructed calorimetric clusters which are treated as massless particles. For the Monte Carlo hadronic events, the global event shape variables are calculated before (particle level) and after (detector level) detector simulation. The calculation before the detector simulation takes into account all stable charged and neutral particles. The ratio of the particle level to the detector level distributions gives bin by bin correction factors that are applied to the measured distributions after background subtraction.

In the case of charged particle multiplicity distribution the detector corrections are obtained using an unfolding matrix and assuming all weakly decaying light particles ( $K_S^0$ ,  $\Lambda$ , etc. with mean lifetime larger than  $3.3 \times 10^{-10}$  s) to be stable. We correct the data for initial and final state photon radiation bin by bin using Monte Carlo distributions at particle level with and without radiation. This correction procedure is sufficiently accurate given the limited statistics of the data sample.

Figure 3 shows the corrected thrust distributions obtained at 161 and 172 GeV. The data are compared with JETSET 7.4 PS [19], HERWIG 5.8 [20], ARIADNE 4.06 [21] and COJETS 6.23 [22] QCD models at particle level without ISR. A similarly good agreement with the four models is also found for the measurements of  $\rho$ ,  $B_T$  and  $B_W$ .

The systematic errors in the distributions of event shape variables arise mainly due to uncertainties in detector calibration and in estimating the background. The effect of detector calibration is studied by changing the definition of reconstructed objects used in the detector to build the observables. Instead of using calorimetric clusters, the analysis has been repeated with objects obtained from a non-linear combination of the energies of charged tracks and calorimetric clusters. The effect due to possible inhomogeneities in the detector response is estimated by comparing the results with those obtained by restricting the events to the central part of the detector where the resolution is better ( $|\cos \theta_T| < 0.7$ , where  $\theta_T$  is the direction of the thrust axis).

The uncertainty on the background composition of the selected event sample has been estimated by repeating the analysis with:

- an alternative criterion to reject the hard initial state photon events based on a cut on the reconstructed effective center of mass energy. The cut corresponds to  $\sqrt{s'/s} > 0.87$ .
- a variation of the  $W^+W^-$  background by  $\pm 12\%$  at 161 GeV or suppressing the  $W^+W^-$  rejection criteria at 172 GeV.
- a variation of the two-photon background by  $\pm 30\%$ .

The final systematic error is taken as the sum in quadrature of all the above mentioned contributions.

# Energy Dependences of the Mean Values

An important test of the QCD models is to check the predicted energy evolution of the event shape variables. The mean values of thrust and charged particle multiplicity obtained in this analysis are shown in figure 4, together with those determined at the Z resonance [18,23], above the Z [6,7,24] and at low energy  $e^+e^-$  machines [25]. Also shown are the energy dependences of these quantities as predicted by JETSET 7.4 PS, JETSET 7.4 ME, HERWIG 5.8, ARIADNE 4.06 and COJETS 6.23 Monte Carlo models with constant parameter values over the entire energy range. These models have been tuned [26] from global event shape distributions and particle multiplicity distributions measured at 91.2 GeV. They use different approaches to describe the perturbative and non-perturbative phase of QCD evolution.

All models are in agreement with the present measurements for the thrust distribution. We also find similar agreement for scaled heavy jet mass and the jet broadening parameters. The situation is different for charged particle multiplicity. The JETSET 7.4 ME model fails to describe the energy dependence of  $\langle n_{ch} \rangle$  over the entire energy range. This is understood as a consequence of a low parton multiplicity before fragmentation in  $\mathcal{O}(\alpha_s^2)$  approximation used in the matrix element calculation. Also COJETS 6.23, which does not include the (predominantly destructive) QCD coherence effect, predicts somewhat larger mean charged particle multiplicity at higher  $\sqrt{s}$  than the observed values. The measured mean values of thrust, scaled heavy jet mass, total jet broadening, wide jet broadening and charged particle multiplicity are summarised in table 2.

## Jet Rates

Jets are reconstructed using the JADE [27] and the Durham [13] algorithms. In the JADE algorithm, for each pair of particles  $i$  and  $j$ , the expression:

$$y_{ij}^J = \frac{2E_i E_j}{s} \cdot (1 - \cos \theta_{ij})$$

is evaluated.  $E_i$  and  $E_j$  are energies of particles  $i$ ,  $j$  and  $\theta_{ij}$  is the angle between them. The pair for which  $y_{ij}$  is smallest is replaced by a pseudo-particle  $l$  with four-momentum

$$p_l = p_i + p_j .$$

This procedure is repeated until all  $y_{ij}$ 's exceed the jet resolution parameter  $y_{cut}$ . The remaining pseudo-particles are called jets.

For the Durham algorithm, a similar procedure is followed using instead the expression for  $y_{ij}$ :

$$y_{ij}^D = \frac{2 \min(E_i^2, E_j^2)}{s} \cdot (1 - \cos \theta_{ij})$$

The jet fraction  $f_n$  is the fraction of all hadronic events containing  $n$ -jets

$$f_n = \frac{\sigma_{n-jets}}{\sigma_{tot}} .$$

$f_n$  is a function of the jet resolution parameter  $y_{cut}$ .

The rate of events with 2, 3, 4 and 5 jets has been measured as a function of the jet resolution parameter. For each value of the resolution parameter  $y_{cut}$ , the jet rates have been corrected for

background contamination and detector effects in the same manner as for the other event shape variables. Figures 5 and 6 show the corrected jet fractions measured at the two energies with the JADE and the Durham algorithms respectively. The errors shown include both statistical and systematic errors added in quadrature. The lines correspond to the prediction of the JETSET 7.4 PS model. Tables 3 and 4 summarise the mean jet rates measured with the two algorithms as a function of  $y_{cut}$ .

## Determination of $\alpha_s$

Resummed leading-log and next-to-leading-log calculations exist for the event shape variables  $T$ ,  $\rho$ ,  $B_T$  and  $B_W$  [14–17]. These calculations have been combined with the complete  $\mathcal{O}(\alpha_s^2)$  QCD calculations giving rise to a reliable description over a large kinematic region. In order to derive  $\alpha_s$ , we fit the measured distributions of these event shape variables to these theoretical calculations. These calculations are done for partons and do not include heavy quark mass effects. To compare the analytical calculations with the experimental distributions, the effects of hadronisation and decays have been incorporated using Monte Carlo programs with standard L3 parameters [26].

For the fit, we use the ranges as given in table 5. The ranges are chosen by taking into account the following factors:

- reliability of the resummation calculation,
- smallness and uniformity of detector and hadronisation corrections,
- sufficient statistics.

Figures 7(a-d) show the experimental data together with the QCD fits for the four variables thrust, scaled heavy jet mass, total and wide jet broadening at 172 GeV. The results on  $\alpha_s$  obtained from the fits at 161 and 172 GeV are summarised in tables 6 and 7 respectively.

The errors are divided into three main parts. The first part corresponds to the statistical errors together with the experimental systematic uncertainties estimated by varying the energy calibration and background content as mentioned earlier. The second part shows the variation in the fitted value of  $\alpha_s$  due to different hadronisation corrections. The hadronisation correction using JETSET with tuned parameter set [26] has been taken as a reference point.  $\alpha_s$  has been determined using hadronisation corrections from different models and by changing the parameter values of JETSET by one standard deviation and not including the effects of Bose-Einstein correlations. For all variables, the most important variation comes from the change in the fragmentation models. We use this as an estimate of the overall hadronisation uncertainty. The third part summarises the errors coming from uncalculated higher orders in the QCD predictions. These errors have been estimated in two independent ways: by varying the renormalisation scale and by changing the matching scheme. The scale error is obtained by repeating the fit for different values of the renormalisation scale in the interval  $0.5\sqrt{s} \leq \mu \leq 2\sqrt{s}$ . For all these scales a good fit is obtained. The matching scheme uncertainty is obtained from half of the maximum spread due to the variation of the matching algorithm. The larger of the two is taken as the theoretical uncertainty due to uncalculated higher orders. The overall theoretical error is obtained by adding to this in quadrature the hadronisation uncertainty.

The  $\alpha_s$  values from the four distributions are affected differently by higher order corrections and hadronisation effects. To obtain a combined value for the strong coupling constant we take the unweighted average of the four  $\alpha_s$  values for each energy. We assign the overall theoretical

uncertainty as the average of the four theoretical errors. The combined results for the two energies are:

$$\begin{aligned}\alpha_s(161 \text{ GeV}) &= 0.103 \pm 0.005 \pm 0.005 \\ \alpha_s(172 \text{ GeV}) &= 0.104 \pm 0.006 \pm 0.005\end{aligned}$$

where the first error is experimental and the second error is theoretical.

This may be compared with our measurements at lower energies [3,6] using the same analysis procedure and variables. The results are:

$$\begin{aligned}\alpha_s(91 \text{ GeV}) &= 0.122 \pm 0.002 \pm 0.007 \\ \alpha_s(133 \text{ GeV}) &= 0.107 \pm 0.005 \pm 0.006\end{aligned}$$

It should be noted that the theoretical errors are strongly correlated between these four measurements. The higher order uncertainties should be the same and the hadronisation corrections should be of similar size at these energies. To study the energy dependence of  $\alpha_s$ , one can therefore consider the variation with errors given by experimental errors alone. Table 8 summarises  $\alpha_s$  values from our measurements at the four center of mass energies, evaluated at the  $m_Z$  scale according to the QCD evolution [28]. It may be noted that the weighted average of the three high energy measurements of  $\alpha_s$  reported in table 8 is  $2.3 \sigma$  below the Z pole value. Since the experimental error is dominantly statistical, future LEP2 measurements will show whether this effect is real or a statistical fluctuation.

The four measurements are shown in figure 8a with experimental errors only together with a fit to QCD evolution function. The fit leads to  $\chi^2$  of 6.0 for three degrees of freedom corresponding to a probability of 0.11. On the other hand, a constant  $\alpha_s$  will give a  $\chi^2$  of 24.7 corresponding to a probability of  $0.2 \times 10^{-4}$ .

Figure 8b summarises the  $\alpha_s$  values measured by L3 from hadronic  $\tau$  decays [4], Z line-shape [29] and event shape distributions at various energies (denoted by Q), together with the QCD prediction obtained from a fit to the event shape measurements only. These measurements support the energy evolution of the strong coupling constant predicted by QCD.

## Acknowledgements

We wish to congratulate the CERN accelerator divisions for the successful upgrade of the LEP machine and to express our gratitude for the good performance of the machine. We acknowledge with appreciation the effort of all engineers, technicians and support staff who have participated in the construction and maintenance of this experiment. Those of us who are not from member states thank CERN for its hospitality and help.

# References

- [1] M. Gell-Mann, Acta Phys. Austriaca Suppl. **IX** (1972) 733;  
H. Fritzsche and M. Gell-Mann, 16th International Conference on High Energy Physics, Batavia, 1972; editors J.D. Jackson and A. Roberts, National Accelerator Laboratory (1972);  
H. Fritzsche, M. Gell-Mann and H. Leytwyler, Phys. Lett. **B 47** (1973) 365;  
D.J. Gross and F. Wilczek, Phys. Rev. Lett. **30** (1973) 1343;  
D.J. Gross and F. Wilczek, Phys. Rev. **D8** (1973) 3633;  
H.D. Politzer, Phys. Rev. Lett. **30** (1973) 1346;  
G. 't Hooft, Nucl. Phys. **B33** (1971) 173.
- [2] T. Hebbeker, Phys. Rep. **Vol.217** (1992) 69;  
S.Bethke, J.E. Pilcher, Ann. Rev. Nucl. Part. Sci. **42** (1992) 251;  
M. Schmelling, Phys. Scr. **51** (1995) 683.
- [3] L3 Collaboration, O. Adriani *et al.*, Phys. Lett. **B284** (1992) 471:  
S. Banerjee, S. Müller, L3 note 1441 (1993)<sup>1</sup>.
- [4] L3 Collaboration, O. Adriani *et al.*, Phys. Rep., **236** (1993) 1.
- [5] ALEPH Collaboration, D. Decamp *et al.*, Phys. Lett. **B284** (1992) 163;  
DELPHI Collaboration, P. Abreu *et al.*, Z. Physik **C59** (1993) 21;  
OPAL Collaboration, P.D. Acton *et al.*, Z. Physik **C59** (1993) 1.
- [6] L3 Collaboration, M.Acciarri *et al.*, Phys. Lett. **B371** (1996) 137.
- [7] ALEPH Collaboration, D. Buskulic *et al.*, Z. Physik. **C73** (1997) 409;  
DELPHI Collaboration, P. Abreu *et al.*, CERN-PPE 96-130, (1996);  
OPAL Collaboration, G. Alexander *et al.*, Z. Physik **C72** (1996) 191.
- [8] L3 Collaboration, B. Adeva *et al.*, Nucl. Inst. Meth. **A 289** (1990) 35;  
L3 Collaboration, M. Acciari *et al.*, Nucl. Inst. Meth. **A 351** (1994) 300.
- [9] PYTHIA 5.7 Monte Carlo Program:  
QCD parton shower and fragmentation process are taken from JETSET 7.4 [19];  
T. Sjöstrand, CERN-TH-7112/93 (1993), revised august 1995;  
T. Sjöstrand, Comp. Phys. Comm. **82** (1994) 74.
- [10] The L3 detector simulation is based on GEANT Version 3.15.  
See R. Brun *et al.*, "GEANT 3", CERN DD/EE/84-1 (Revised), September 1987.  
The GHEISHA program (H. Fesefeldt, RWTH Aachen Report PITHA 85/02 (1985)) is used to simulate hadronic interactions.
- [11] KORALW Monte Carlo Program:  
M. Skrzypek *et al*, Comp. Phys. Comm. **94** (1996) 216;  
M. Skrzypek *et al*, Phys. Lett. **B372** (1996) 289.
- [12] G.A. Schuler and T. Sjöstrand, Nucl. Phys. **B407** (1993) 539; Phys. Lett. **B300** (1993) 169.  
The Monte Carlo program used for two-photon processes is incorporated in PYTHIA 5.7 [9].



- [13] Y.L. Dokshitzer, Contribution to the Workshop on Jets at LEP and HERA (1990);  
N. Brown and W.J. Stirling, Rutherford Preprint RAL-91-049;  
S. Catani *et al.*, Phys. Lett. **B269** (1991) 432;  
S. Bethke *et al.*, Nucl. Phys. **B370** (1992) 310.
- [14] S. Catani *et al.*, Phys. Lett. **B263** (1991) 491.
- [15] S. Catani *et al.*, Phys. Lett. **B272** (1991) 360.
- [16] S. Catani *et al.*, Phys. Lett. **B295** (1992) 269.
- [17] S. Bethke *et al.*, Nucl. Phys. **B370** (1992) 310.
- [18] L3 Collaboration, B. Adeva *et al.*, Z. Phys. **C55** (1992) 39.
- [19] JETSET 7.4 Monte Carlo Program:  
T. Sjöstrand, Comp. Phys. Comm. **39** (1986) 347;  
T. Sjöstrand and M. Bengtsson, Comp. Phys. Comm. **43** (1987) 367.
- [20] HERWIG 5.6 Monte Carlo Program:  
G. Marchesini and B. Webber, Nucl. Phys. **B310** (1988) 461;  
I.G. Knowles, Nucl. Phys. **B310** (1988) 571;  
G. Marchesini *et al.*, Comp. Phys. Comm. **67** (1992) 465.
- [21] ARIADNE 4.06 Monte Carlo Program:  
U. Pettersson, “ARIADNE: A Monte Carlo for QCD Cascades in the Color Dipole Formulation”, Lund Preprint, LU TP 88-5 (1988);  
L. Lönnblad, “The Colour Dipole Cascade Model and the Ariadne Program”, Lund Preprint, LU TP 91-11 (1991).
- [22] COJETS 6.23 Monte Carlo Program:  
R. Odorico, Nucl. Phys. **B228** (1983) 381;  
R. Odorico, Comp. Phys. Comm. **32** (1984) 139, Erratum: **34** (1985) 43;  
R. Mazzanti and R. Odorico, Nucl. Phys. **B370** (1992) 23; Bologna preprint DFUB 92/1.
- [23] ALEPH Collaboration, D. Decamp *et al.*, Phys. Lett. **B273** (1991) 181;  
DELPHI Collaboration, P. Aarnio *et al.*, Phys. Lett. **B240** (1990) 271;  
DELPHI Collaboration, P. Abreu *et al.*, Z. Phys. **C50** (1991) 185;  
OPAL Collaboration, M.Z. Akrawy *et al.*, Z. Phys. **C47** (1990) 505;  
OPAL Collaboration, P.D. Acton *et al.*, Z. Phys. **C53** (1992) 539.
- [24] OPAL Collaboration, G. Alexander *et al.*, CERN-PPE 97-15, (1997).
- [25] AMY Collaboration, Y.K. Li *et al.*, Phys. Rev. **D41** (1990) 2675;  
AMY Collaboration, H.W. Zheng *et al.*, Phys. Rev. **D42** (1990) 737;  
JADE Collaboration, W. Bartel *et al.*, Z. Phys. **C20** (1983) 187;  
MARK J Collaboration, D.P. Barber *et al.*, Phys. Rev. Lett. **43** (1979) 901;  
TASSO Collaboration, W. Braunschweig *et al.*, Z. Phys. **C45** (1989) 193;  
TASSO Collaboration, W. Braunschweig *et al.*, Z. Phys. **C47** (1990) 187;  
M. Yamauchi (TOPAZ Collaboration), Contribution to the 24th Int. Conf. on High Energy Physics, Munich (1988).

- [26] S. Banerjee, S. Banerjee, L3 note 1978 (1996) <sup>1)</sup>
- [27] JADE Collaboration, W. Bartel *et al.*, Z. Phys. **C33** (1986) 23;  
JADE Collaboration, S. Bethke *et al.*, Phys. Lett. **B213** (1988) 235.
- [28] Particle Data Group, R.M. Barnett *et al.*, Phys. Rev. **D54** (1996) 77.
- [29] L3 Collaboration, M. Acciarri *et al.*, Z. Phys. **C62** (1994) 551.

---

<sup>1)</sup>These L3 Internal Notes are freely available on request from: The L3 secretariat, CERN, CH-1211 Geneva 23, Switzerland.

## The L3 Collaboration:

M. Acciarri,<sup>29</sup> O. Adriani,<sup>18</sup> M. Aguilar-Benitez,<sup>28</sup> S. Ahlen,<sup>12</sup> J. Alcaraz,<sup>28</sup> G. Alemani,<sup>24</sup> J. Allaby,<sup>19</sup> A. Aloisio,<sup>31</sup> G. Alverson,<sup>13</sup> M.G. Alviggi,<sup>31</sup> G. Ambrosi,<sup>21</sup> H. Anderhub,<sup>51</sup> V.P. Andreev,<sup>7,40</sup> T. Angelescu,<sup>14</sup> F. Anselmo,<sup>10</sup> A. Arefiev,<sup>30</sup> T. Azemoon,<sup>3</sup> T. Aziz,<sup>11</sup> P. Bagnaia,<sup>39</sup> L. Baksay,<sup>46</sup> S. Banerjee,<sup>11</sup> Sw. Banerjee,<sup>11</sup> K. Banicz,<sup>48</sup> A. Barczyk,<sup>51,ϕ</sup> R. Barillère,<sup>19</sup> L. Barone,<sup>39</sup> P. Bartalini,<sup>36</sup> A. Baschirotto,<sup>29</sup> M. Basile,<sup>10</sup> R. Battiston,<sup>36</sup> A. Bay,<sup>24</sup> F. Becattini,<sup>18</sup> U. Becker,<sup>17</sup> F. Behner,<sup>51</sup> J. Berdugo,<sup>28</sup> P. Berges,<sup>17</sup> B. Bertucci,<sup>36</sup> B.L. Betev,<sup>51</sup> S. Bhattacharya,<sup>11</sup> M. Biasini,<sup>19</sup> A. Biland,<sup>51</sup> G.M. Bilei,<sup>36</sup> J.J. Blaising,<sup>4</sup> S.C. Blyth,<sup>37</sup> G.J. Bobbink,<sup>2</sup> R. Bock,<sup>1</sup> A. Böhm,<sup>1</sup> L. Boldizar,<sup>15</sup> B. Borgia,<sup>39</sup> D. Bourilkov,<sup>51</sup> M. Bourquin,<sup>21</sup> S. Braccini,<sup>21</sup> J.G. Branson,<sup>42</sup> V. Brigljevic,<sup>51</sup> I.C. Brock,<sup>37</sup> A. Buffini,<sup>18</sup> A. Buijs,<sup>47</sup> J.D. Burger,<sup>17</sup> W.J. Burger,<sup>21</sup> J. Busenitz,<sup>46</sup> A. Button,<sup>3</sup> X.D. Cai,<sup>17</sup> M. Campanelli,<sup>51</sup> M. Capell,<sup>17</sup> G. Cara Romeo,<sup>10</sup> G. Carlino,<sup>31</sup> A.M. Cartacci,<sup>18</sup> J. Casaus,<sup>28</sup> G. Castellini,<sup>18</sup> F. Cavallari,<sup>39</sup> N. Cavallo,<sup>31</sup> C. Cecchi,<sup>21</sup> M. Cerrada,<sup>28</sup> F. Cesaroni,<sup>25</sup> M. Chamiz,<sup>28</sup> Y.H. Chang,<sup>53</sup> U.K. Chaturvedi,<sup>20</sup> S.V. Chekanov,<sup>33</sup> M. Chemarin,<sup>27</sup> A. Chen,<sup>53</sup> G. Chen,<sup>8</sup> G.M. Chen,<sup>8</sup> H.F. Chen,<sup>22</sup> H.S. Chen,<sup>8</sup> X. Chereau,<sup>4</sup> G. Chiefari,<sup>31</sup> C.Y. Chien,<sup>5</sup> L. Cifarelli,<sup>41</sup> F. Cindolo,<sup>10</sup> C. Cividini,<sup>18</sup> I.M. Clare,<sup>17</sup> R. Clare,<sup>17</sup> H.O. Cohn,<sup>34</sup> G. Coignet,<sup>4</sup> A.P. Colijn,<sup>2</sup> N. Colino,<sup>28</sup> V. Commichau,<sup>1</sup> S. Costantini,<sup>9</sup> F. Cotorobai,<sup>14</sup> B. de la Cruz,<sup>28</sup> A. Csilling,<sup>15</sup> T.S. Dai,<sup>17</sup> R.D. Alessandro,<sup>18</sup> R. de Asmundis,<sup>31</sup> A. Degré,<sup>4</sup> K. Deiters,<sup>49</sup> D. della Volpe,<sup>31</sup> P. Denes,<sup>38</sup> F. DeNotaristefani,<sup>39</sup> D. DiBitonto,<sup>46</sup> M. Diemoz,<sup>39</sup> D. van Dierendonck,<sup>2</sup> F. Di Lodovico,<sup>51</sup> C. Dionisi,<sup>39</sup> M. Dittmar,<sup>51</sup> A. Dominguez,<sup>42</sup> A. Doria,<sup>31</sup> M.T. Dova,<sup>2,ϕ</sup> D. Duchesneau,<sup>4</sup> P. Duinker,<sup>2</sup> I. Duran,<sup>43</sup> S. Dutta,<sup>11</sup> S. Easo,<sup>36</sup> Yu. Efremenko,<sup>34</sup> H. El Mamouni,<sup>27</sup> A. Engler,<sup>37</sup> F.J. Eppling,<sup>17</sup> F.C. Erné,<sup>2</sup> J.P. Ernenwein,<sup>27</sup> P. Extermann,<sup>21</sup> M. Fabre,<sup>49</sup> R. Faccini,<sup>39</sup> S. Falciano,<sup>39</sup> A. Favara,<sup>18</sup> J. Fay,<sup>27</sup> O. Fedin,<sup>40</sup> M. Felcini,<sup>51</sup> B. Fenyi,<sup>46</sup> T. Ferguson,<sup>37</sup> F. Ferroni,<sup>39</sup> H. Fesefeldt,<sup>1</sup> E. Fiandrini,<sup>36</sup> J.H. Field,<sup>21</sup> F. Filthaut,<sup>37</sup> P.H. Fisher,<sup>17</sup> I. Fisk,<sup>42</sup> G. Forconi,<sup>17</sup> L. Fredj,<sup>21</sup> K. Freudenreich,<sup>51</sup> C. Furetta,<sup>29</sup> Yu. Galaktionov,<sup>30,17</sup> S.N. Ganguli,<sup>11</sup> P. Garcia-Abia,<sup>50</sup> S.S. Gau,<sup>13</sup> S. Gentile,<sup>39</sup> N. Gheordanescu,<sup>14</sup> S. Giagu,<sup>39</sup> S. Goldfarb,<sup>24</sup> J. Goldstein,<sup>12</sup> Z.F. Gong,<sup>22</sup> A. Gougas,<sup>5</sup> G. Gratta,<sup>35</sup> M.W. Gruenewald,<sup>9</sup> V.K. Gupta,<sup>38</sup> A. Gurtu,<sup>11</sup> L.J. Gutay,<sup>48</sup> B. Hartmann,<sup>1</sup> A. Hasan,<sup>32</sup> D. Hatzifotiadou,<sup>10</sup> T. Hebbeker,<sup>9</sup> A. Hervé,<sup>19</sup> W.C. van Hoek,<sup>33</sup> H. Hofer,<sup>51</sup> S.J. Hong,<sup>45</sup> H. Hoorani,<sup>37</sup> S.R. Hou,<sup>53</sup> G. Hu,<sup>5</sup> V. Innocenti,<sup>9</sup> K. Jenkes,<sup>1</sup> B.N. Jin,<sup>8</sup> L.W. Jones,<sup>3</sup> P. de Jong,<sup>19</sup> I. Josa-Mutuberria,<sup>28</sup> A. Kasser,<sup>24</sup> R.A. Khan,<sup>20</sup> D. Kamrad,<sup>50</sup> Yu. Kamyshkov,<sup>34</sup> J.S. Kapustinsky,<sup>26</sup> Y. Karyotakis,<sup>4</sup> M. Kaur,<sup>20,ϕ</sup> M.N. Kienzle-Focacci,<sup>21</sup> D. Kim,<sup>39</sup> D.H. Kim,<sup>45</sup> J.K. Kim,<sup>45</sup> S.C. Kim,<sup>45</sup> Y.G. Kim,<sup>45</sup> W.W. Kinnison,<sup>26</sup> A. Kirkby,<sup>35</sup> D. Kirkby,<sup>35</sup> J. Kirkby,<sup>19</sup> D. Kiss,<sup>15</sup> W. Kittel,<sup>33</sup> A. Klimentov,<sup>17,30</sup> A.C. König,<sup>33</sup> A. Kopp,<sup>50</sup> I. Korolko,<sup>30</sup> V. Koutsenko,<sup>17,30</sup> R.W. Kraemer,<sup>37</sup> W. Krenz,<sup>1</sup> A. Kunin,<sup>17,30</sup> P. Ladron de Guevara,<sup>28</sup> I. Laktineh,<sup>27</sup> G. Landi,<sup>18</sup> C. Lapoint,<sup>17</sup> K. Lassila-Perini,<sup>51</sup> P. Laurikainen,<sup>23</sup> M. Lebeau,<sup>19</sup> A. Lebedev,<sup>17</sup> P. Lebrun,<sup>27</sup> P. Lecomte,<sup>51</sup> P. Lecoq,<sup>19</sup> P. Le Coultre,<sup>51</sup> J.M. Le Goff,<sup>19</sup> R. Leiste,<sup>50</sup> E. Leonardi,<sup>39</sup> P. Levchenko,<sup>40</sup> C. Li,<sup>22</sup> C.H. Lin,<sup>53</sup> W.T. Lin,<sup>53</sup> F.L. Linde,<sup>2,19</sup> L. Lista,<sup>31</sup> Z.A. Liu,<sup>8</sup> W. Lohmann,<sup>50</sup> E. Longo,<sup>39</sup> W. Lu,<sup>35</sup> Y.S. Lu,<sup>8</sup> K. Lübelmeyer,<sup>1</sup> C. Luci,<sup>39</sup> D. Luckey,<sup>17</sup> L. Luminari,<sup>39</sup> W. Lustermann,<sup>49</sup> W.G. Ma,<sup>22</sup> M. Maity,<sup>11</sup> G. Majumder,<sup>11</sup> L. Malgeri,<sup>39</sup> A. Malinin,<sup>30</sup> C. Mañá,<sup>28</sup> D. Mangeol,<sup>33</sup> S. Mangla,<sup>11</sup> P. Marchesini,<sup>51</sup> A. Marin,<sup>12</sup> J.P. Martin,<sup>27</sup> F. Marzano,<sup>39</sup> G.G.G. Massaro,<sup>2</sup> D. McNally,<sup>19</sup> R.R. McNeil,<sup>7</sup> S. Mele,<sup>31</sup> L. Merola,<sup>31</sup> M. Meschini,<sup>18</sup> W.J. Metzger,<sup>33</sup> M. von der Mey,<sup>1</sup> Y. Mi,<sup>24</sup> A. Mihul,<sup>14</sup> A.J.W. van Mil,<sup>33</sup> G. Mirabelli,<sup>39</sup> J. Mnich,<sup>19</sup> P. Molnar,<sup>9</sup> B. Monteleoni,<sup>18</sup> R. Moore,<sup>3</sup> S. Morganti,<sup>39</sup> T. Moulik,<sup>11</sup> R. Mount,<sup>35</sup> S. Müller,<sup>1</sup> F. Muheim,<sup>21</sup> A.J.M. Muijs,<sup>2</sup> S. Nahn,<sup>17</sup> M. Napolitano,<sup>31</sup> F. Nessi-Tedaldi,<sup>51</sup> H. Newman,<sup>35</sup> T. Niessen,<sup>1</sup> A. Nippe,<sup>1</sup> A. Nisati,<sup>39</sup> H. Nowak,<sup>50</sup> Y.D. Oh,<sup>45</sup> H. Opitez,<sup>1</sup> G. Organtini,<sup>39</sup> R. Ostonen,<sup>23</sup> C. Palomares,<sup>28</sup> D. Pandoulas,<sup>1</sup> S. Paoletti,<sup>39</sup> P. Paolucci,<sup>31</sup> H.K. Park,<sup>37</sup> I.H. Park,<sup>45</sup> G. Pascale,<sup>39</sup> G. Passaleva,<sup>18</sup> S. Patricelli,<sup>31</sup> T. Paul,<sup>13</sup> M. Pauluzzi,<sup>36</sup> C. Paus,<sup>1</sup> F. Pauss,<sup>51</sup> D. Peach,<sup>19</sup> Y.J. Pei,<sup>1</sup> S. Pensotti,<sup>29</sup> D. Perret-Gallix,<sup>4</sup> B. Petersen,<sup>33</sup> S. Petrak,<sup>9</sup> A. Pevsner,<sup>5</sup> D. Piccolo,<sup>31</sup> M. Pieri,<sup>18</sup> J.C. Pinto,<sup>37</sup> P.A. Piroué,<sup>38</sup> E. Pistolesi,<sup>29</sup> V. Plyaskin,<sup>30</sup> M. Pohl,<sup>51</sup> V. Pojidaev,<sup>30,18</sup> H. Postema,<sup>17</sup> N. Produit,<sup>21</sup> D. Prokofiev,<sup>40</sup> G. Rahal-Callot,<sup>51</sup> N. Raja,<sup>11</sup> P.G. Rancoita,<sup>29</sup> M. Rattaggi,<sup>29</sup> G. Raven,<sup>42</sup> P. Razis,<sup>32</sup> K. Read,<sup>34</sup> D. Ren,<sup>51</sup> M. Rescigno,<sup>39</sup> S. Reucroft,<sup>13</sup> T. van Rhee,<sup>47</sup> S. Riemann,<sup>50</sup> K. Riles,<sup>3</sup> A. Robohm,<sup>51</sup> J. Rodin,<sup>17</sup> B.P. Roe,<sup>3</sup> L. Romero,<sup>28</sup> S. Rosier-Lees,<sup>4</sup> Ph. Rossetet,<sup>24</sup> W. van Rossum,<sup>47</sup> S. Roth,<sup>1</sup> J.A. Rubio,<sup>19</sup> D. Ruschmeier,<sup>9</sup> H. Rykaczewski,<sup>51</sup> J. Salicio,<sup>19</sup> E. Sanchez,<sup>28</sup> M.P. Sanders,<sup>33</sup> M.E. Sarakinos,<sup>23</sup> S. Sarkar,<sup>11</sup> M. Sassowsky,<sup>1</sup> C. Schäfer,<sup>1</sup> V. Schegelsky,<sup>40</sup> S. Schmidt-Kaerst,<sup>1</sup> D. Schmitz,<sup>1</sup> P. Schmitz,<sup>1</sup> N. Scholz,<sup>51</sup> H. Schopper,<sup>52</sup> D.J. Schotanus,<sup>33</sup> J. Schwenke,<sup>1</sup> G. Schwing,<sup>1</sup> C. Sciacca,<sup>31</sup> D. Sciarino,<sup>21</sup> L. Servoli,<sup>36</sup> S. Shevchenko,<sup>35</sup> N. Shivarov,<sup>44</sup> V. Shoutko,<sup>30</sup> J. Shukla,<sup>26</sup> E. Shumilov,<sup>30</sup> A. Shvorob,<sup>35</sup> T. Siedenburt,<sup>1</sup> D. Son,<sup>45</sup> A. Sopczak,<sup>50</sup> B. Smith,<sup>17</sup> P. Spillantini,<sup>18</sup> M. Steuer,<sup>17</sup> D.P. Stickland,<sup>38</sup> A. Stone,<sup>7</sup> H. Stone,<sup>38</sup> B. Stoyanov,<sup>44</sup> A. Straessner,<sup>1</sup> K. Strauch,<sup>16</sup> K. Sudhakar,<sup>11</sup> G. Sultanov,<sup>20</sup> L.Z. Sun,<sup>22</sup> G.F. Susinno,<sup>21</sup> H. Suter,<sup>51</sup> J.D. Swain,<sup>20</sup> X.W. Tang,<sup>8</sup> L. Tauscher,<sup>6</sup> L. Taylor,<sup>13</sup> Samuel C.C. Ting,<sup>17</sup> S.M. Ting,<sup>17</sup> M. Tonutti,<sup>1</sup> S.C. Tonwar,<sup>11</sup> J. Tóth,<sup>15</sup> C. Tully,<sup>38</sup> H. Tuchscherer,<sup>46</sup> K.L. Tung,<sup>8</sup> Y. Uchida,<sup>17</sup> J. Ulbricht,<sup>51</sup> U. Uwer,<sup>19</sup> E. Valente,<sup>39</sup> R.T. Van de Walle,<sup>33</sup> G. Vesztegombi,<sup>15</sup> I. Vetlitsky,<sup>30</sup> G. Viertel,<sup>51</sup> M. Vivargent,<sup>4</sup> R. Völkert,<sup>50</sup> H. Vogel,<sup>37</sup> H. Vogt,<sup>50</sup> I. Vorobiev,<sup>30</sup> A.A. Vorobyov,<sup>40</sup> A. Vorvolakos,<sup>32</sup> M. Wadhwa,<sup>6</sup> W. Wallraff,<sup>1</sup> J.C. Wang,<sup>17</sup> X.L. Wang,<sup>22</sup> Z.M. Wang,<sup>22</sup> A. Weber,<sup>1</sup> F. Wittgenstein,<sup>19</sup> S.X. Wu,<sup>20</sup> S. Wynnhoff,<sup>1</sup> J. Xu,<sup>12</sup> Z.Z. Xu,<sup>22</sup> B.Z. Yang,<sup>22</sup> C.G. Yang,<sup>8</sup> X.Y. Yao,<sup>8</sup> J.B. Ye,<sup>22</sup> S.C. Yeh,<sup>53</sup> J.M. You,<sup>37</sup> An. Zalite,<sup>40</sup> Yu. Zalite,<sup>40</sup> P. Zemp,<sup>51</sup> Y. Zeng,<sup>1</sup> Z. Zhang,<sup>8</sup> Z.P. Zhang,<sup>22</sup> B. Zhou,<sup>12</sup> G.Y. Zhu,<sup>8</sup> R.Y. Zhu,<sup>35</sup> A. Zichichi,<sup>10,19,20</sup> F. Ziegler,<sup>50</sup>

- 1 I. Physikalisches Institut, RWTH, D-52056 Aachen, FRG<sup>§</sup>  
III. Physikalisches Institut, RWTH, D-52056 Aachen, FRG<sup>§</sup>
  - 2 National Institute for High Energy Physics, NIKHEF, and University of Amsterdam, NL-1009 DB Amsterdam, The Netherlands
  - 3 University of Michigan, Ann Arbor, MI 48109, USA
  - 4 Laboratoire d'Annecy-le-Vieux de Physique des Particules, LAPP, IN2P3-CNRS, BP 110, F-74941 Annecy-le-Vieux CEDEX, France
  - 5 Johns Hopkins University, Baltimore, MD 21218, USA
  - 6 Institute of Physics, University of Basel, CH-4056 Basel, Switzerland
  - 7 Louisiana State University, Baton Rouge, LA 70803, USA
  - 8 Institute of High Energy Physics, IHEP, 100039 Beijing, China<sup>△</sup>
  - 9 Humboldt University, D-10099 Berlin, FRG<sup>§</sup>
  - 10 University of Bologna and INFN-Sezione di Bologna, I-40126 Bologna, Italy
  - 11 Tata Institute of Fundamental Research, Bombay 400 005, India
  - 12 Boston University, Boston, MA 02215, USA
  - 13 Northeastern University, Boston, MA 02115, USA
  - 14 Institute of Atomic Physics and University of Bucharest, R-76900 Bucharest, Romania
  - 15 Central Research Institute for Physics of the Hungarian Academy of Sciences, H-1525 Budapest 114, Hungary<sup>‡</sup>
  - 16 Harvard University, Cambridge, MA 02139, USA
  - 17 Massachusetts Institute of Technology, Cambridge, MA 02139, USA
  - 18 INFN Sezione di Firenze and University of Florence, I-50125 Florence, Italy
  - 19 European Laboratory for Particle Physics, CERN, CH-1211 Geneva 23, Switzerland
  - 20 World Laboratory, FBLJA Project, CH-1211 Geneva 23, Switzerland
  - 21 University of Geneva, CH-1211 Geneva 4, Switzerland
  - 22 Chinese University of Science and Technology, USTC, Hefei, Anhui 230 029, China<sup>△</sup>
  - 23 SEFT, Research Institute for High Energy Physics, P.O. Box 9, SF-00014 Helsinki, Finland
  - 24 University of Lausanne, CH-1015 Lausanne, Switzerland
  - 25 INFN-Sezione di Lecce and Università Degli Studi di Lecce, I-73100 Lecce, Italy
  - 26 Los Alamos National Laboratory, Los Alamos, NM 87544, USA
  - 27 Institut de Physique Nucléaire de Lyon, IN2P3-CNRS, Université Claude Bernard, F-69622 Villeurbanne, France
  - 28 Centro de Investigaciones Energeticas, Medioambientales y Tecnológicas, CIEMAT, E-28040 Madrid, Spain<sup>b</sup>
  - 29 INFN-Sezione di Milano, I-20133 Milan, Italy
  - 30 Institute of Theoretical and Experimental Physics, ITEP, Moscow, Russia
  - 31 INFN-Sezione di Napoli and University of Naples, I-80125 Naples, Italy
  - 32 Department of Natural Sciences, University of Cyprus, Nicosia, Cyprus
  - 33 University of Nijmegen and NIKHEF, NL-6525 ED Nijmegen, The Netherlands
  - 34 Oak Ridge National Laboratory, Oak Ridge, TN 37831, USA
  - 35 California Institute of Technology, Pasadena, CA 91125, USA
  - 36 INFN-Sezione di Perugia and Università Degli Studi di Perugia, I-06100 Perugia, Italy
  - 37 Carnegie Mellon University, Pittsburgh, PA 15213, USA
  - 38 Princeton University, Princeton, NJ 08544, USA
  - 39 INFN-Sezione di Roma and University of Rome, "La Sapienza", I-00185 Rome, Italy
  - 40 Nuclear Physics Institute, St. Petersburg, Russia
  - 41 University and INFN, Salerno, I-84100 Salerno, Italy
  - 42 University of California, San Diego, CA 92093, USA
  - 43 Dept. de Física de Partículas Elementales, Univ. de Santiago, E-15706 Santiago de Compostela, Spain
  - 44 Bulgarian Academy of Sciences, Central Lab. of Mechatronics and Instrumentation, BU-1113 Sofia, Bulgaria
  - 45 Center for High Energy Physics, Korea Adv. Inst. of Sciences and Technology, 305-701 Taejeon, Republic of Korea
  - 46 University of Alabama, Tuscaloosa, AL 35486, USA
  - 47 Utrecht University and NIKHEF, NL-3584 CB Utrecht, The Netherlands
  - 48 Purdue University, West Lafayette, IN 47907, USA
  - 49 Paul Scherrer Institut, PSI, CH-5232 Villigen, Switzerland
  - 50 DESY-Institut für Hochenergiephysik, D-15738 Zeuthen, FRG
  - 51 Eidgenössische Technische Hochschule, ETH Zürich, CH-8093 Zürich, Switzerland
  - 52 University of Hamburg, D-22761 Hamburg, FRG
  - 53 High Energy Physics Group, Taiwan, China
- <sup>§</sup> Supported by the German Bundesministerium für Bildung, Wissenschaft, Forschung und Technologie  
<sup>‡</sup> Supported by the Hungarian OTKA fund under contract numbers T14459 and T24011.  
<sup>b</sup> Supported also by the Comisión Interministerial de Ciencia y Tecnología  
<sup>‡</sup> Also supported by CONICET and Universidad Nacional de La Plata, CC 67, 1900 La Plata, Argentina  
<sup>◇</sup> Also supported by Panjab University, Chandigarh-160014, India  
<sup>△</sup> Supported by the National Natural Science Foundation of China.

	$\sqrt{s} = 161 \text{ GeV}$	$\sqrt{s} = 172 \text{ GeV}$
ISR $\geq 30 \text{ GeV}$	11.4%	8.5%
$e^+e^- \rightarrow W^+W^- \rightarrow \text{ffff}$	4.4%	8.9%
$e^+e^- \rightarrow e^+e^- + \text{hadrons}$	3.3%	2.8%
$e^+e^- \rightarrow ZZ \rightarrow \text{ffff}$	0.6%	0.5%
$e^+e^- \rightarrow Ze^+e^- \rightarrow e^+e^- \text{ff}$	0.35%	0.35%
$e^+e^- \rightarrow \tau\tau$	0.23%	0.23%

Table 1: Background fraction estimated from Monte Carlo in the selected event samples.

	$\sqrt{s} = 161 \text{ GeV}$	$\sqrt{s} = 172 \text{ GeV}$
$\langle T \rangle$	$0.9457 \pm 0.0031 \pm 0.0017$	$0.9493 \pm 0.0031 \pm 0.0019$
$\langle \rho \rangle$	$0.0436 \pm 0.0025 \pm 0.0009$	$0.0411 \pm 0.0026 \pm 0.0010$
$\langle B_T \rangle$	$0.0946 \pm 0.0031 \pm 0.0018$	$0.0894 \pm 0.0034 \pm 0.0028$
$\langle B_W \rangle$	$0.0683 \pm 0.0026 \pm 0.0014$	$0.0647 \pm 0.0028 \pm 0.0012$
$\langle n_{ch} \rangle$	$25.45 \pm 0.38 \pm 0.32$	$26.61 \pm 0.47 \pm 0.30$

Table 2: Mean values of thrust,  $T$ , scaled heavy jet mass,  $\rho$ , total jet broadening,  $B_T$ , wide jet broadening,  $B_W$  and charged particle multiplicity,  $n_{ch}$ . The first error is statistical and the second is systematic.

$y_{cut}^J$	$\langle n_{jet} \rangle$ (161 GeV)	$\langle n_{jet} \rangle$ (172 GeV)
.010	$2.749 \pm .036 \pm .041$	$2.873 \pm .044 \pm .055$
.020	$2.522 \pm .031 \pm .053$	$2.546 \pm .034 \pm .071$
.040	$2.342 \pm .025 \pm .018$	$2.303 \pm .027 \pm .060$
.060	$2.261 \pm .024 \pm .022$	$2.193 \pm .021 \pm .080$
.080	$2.190 \pm .020 \pm .019$	$2.140 \pm .020 \pm .043$
.100	$2.131 \pm .018 \pm .019$	$2.108 \pm .018 \pm .027$
.120	$2.099 \pm .016 \pm .029$	$2.091 \pm .017 \pm .016$
.140	$2.080 \pm .014 \pm .020$	$2.058 \pm .013 \pm .015$
.160	$2.056 \pm .012 \pm .019$	$2.040 \pm .011 \pm .018$
.180	$2.040 \pm .011 \pm .014$	$2.025 \pm .009 \pm .011$

Table 3: Average jet multiplicity using the JADE algorithm at 161 GeV and 172 GeV.

$y_{cut}^D$	$\langle n_{jet} \rangle$ (161 GeV)	$\langle n_{jet} \rangle$ (172 GeV)
.001	$3.210 \pm .051 \pm .072$	$3.135 \pm .053 \pm .144$
.002	$2.901 \pm .043 \pm .092$	$2.855 \pm .048 \pm .078$
.004	$2.622 \pm .037 \pm .047$	$2.654 \pm .043 \pm .061$
.008	$2.425 \pm .029 \pm .038$	$2.339 \pm .027 \pm .141$
.020	$2.257 \pm .024 \pm .042$	$2.263 \pm .030 \pm .061$
.040	$2.145 \pm .019 \pm .019$	$2.127 \pm .017 \pm .054$
.060	$2.097 \pm .016 \pm .010$	$2.085 \pm .016 \pm .036$
.100	$2.061 \pm .013 \pm .011$	$2.037 \pm .011 \pm .018$
.140	$2.025 \pm .008 \pm .013$	$2.014 \pm .007 \pm .008$

Table 4: Average jet multiplicity using the Durham algorithm at 161 GeV and 172 GeV.

Variable	Fit range
$(1 - T)$	0.00 – 0.30
$\rho$	0.00 – 0.20
$B_T$	0.00 – 0.25
$B_W$	0.00 – 0.20

Table 5: Ranges used for QCD fits to the data

	$(1 - T)$	$\rho$	$B_T$	$B_W$
$\alpha_s(161 \text{ GeV})$	0.102	0.101	0.109	0.099
$\chi^2/\text{d.o.f.}$	1.44	0.83	0.97	1.33
Statistical error	$\pm 0.005$	$\pm 0.005$	$\pm 0.004$	$\pm 0.004$
Systematic error	$\pm 0.004$	$\pm 0.002$	$\pm 0.004$	$\pm 0.002$
Overall experimental error	$\pm 0.006$	$\pm 0.005$	$\pm 0.006$	$\pm 0.004$
Fragmentation Model	$\pm 0.003$	$\pm 0.002$	$\pm 0.001$	$\pm 0.001$
Model parameters	$\pm 0.002$	$\pm 0.002$	$\pm 0.001$	$\pm 0.001$
Hadronisation uncertainty	$\pm 0.003$	$\pm 0.002$	$\pm 0.001$	$\pm 0.001$
QCD scale uncertainty	$\pm 0.004$	$\pm 0.003$	$\pm 0.006$	$\pm 0.003$
Matching scheme uncertainty	$\pm 0.002$	$\pm 0.002$	$\pm 0.005$	$\pm 0.005$
Error due to higher orders	$\pm 0.004$	$\pm 0.003$	$\pm 0.006$	$\pm 0.005$
Overall theoretical error	$\pm 0.005$	$\pm 0.004$	$\pm 0.006$	$\pm 0.005$

Table 6:  $\alpha_s(161 \text{ GeV})$  from the fits to the event shape variables

	$(1 - T)$	$\rho$	$B_T$	$B_W$
$\alpha_s(172 \text{ GeV})$	0.108	0.104	0.106	0.099
$\chi^2/\text{d.o.f.}$	0.28	0.89	1.12	1.08
Statistical error	$\pm 0.005$	$\pm 0.005$	$\pm 0.004$	$\pm 0.004$
Systematic error	$\pm 0.003$	$\pm 0.003$	$\pm 0.003$	$\pm 0.003$
Overall experimental error	$\pm 0.006$	$\pm 0.006$	$\pm 0.005$	$\pm 0.005$
Fragmentation Model	$\pm 0.003$	$\pm 0.002$	$\pm 0.003$	$\pm 0.001$
Model parameters	$\pm 0.002$	$\pm 0.002$	$\pm 0.001$	$\pm 0.001$
Hadronisation uncertainty	$\pm 0.003$	$\pm 0.002$	$\pm 0.003$	$\pm 0.001$
QCD scale uncertainty	$\pm 0.004$	$\pm 0.003$	$\pm 0.005$	$\pm 0.005$
Matching scheme uncertainty	$\pm 0.002$	$\pm 0.003$	$\pm 0.005$	$\pm 0.005$
Error due to higher orders	$\pm 0.004$	$\pm 0.003$	$\pm 0.005$	$\pm 0.005$
Overall theoretical error	$\pm 0.005$	$\pm 0.004$	$\pm 0.006$	$\pm 0.005$

Table 7:  $\alpha_s(172 \text{ GeV})$  from the fits to the event shape variables

$\sqrt{s}$	$\alpha_s(m_Z)$
91 GeV	$0.122 \pm 0.002$
133 GeV	$0.113 \pm 0.006$
161 GeV	$0.111 \pm 0.006$
172 GeV	$0.114 \pm 0.007$

Table 8: The measured  $\alpha_s$  values evolved to the  $m_Z$  scale. The quoted errors are experimental only.

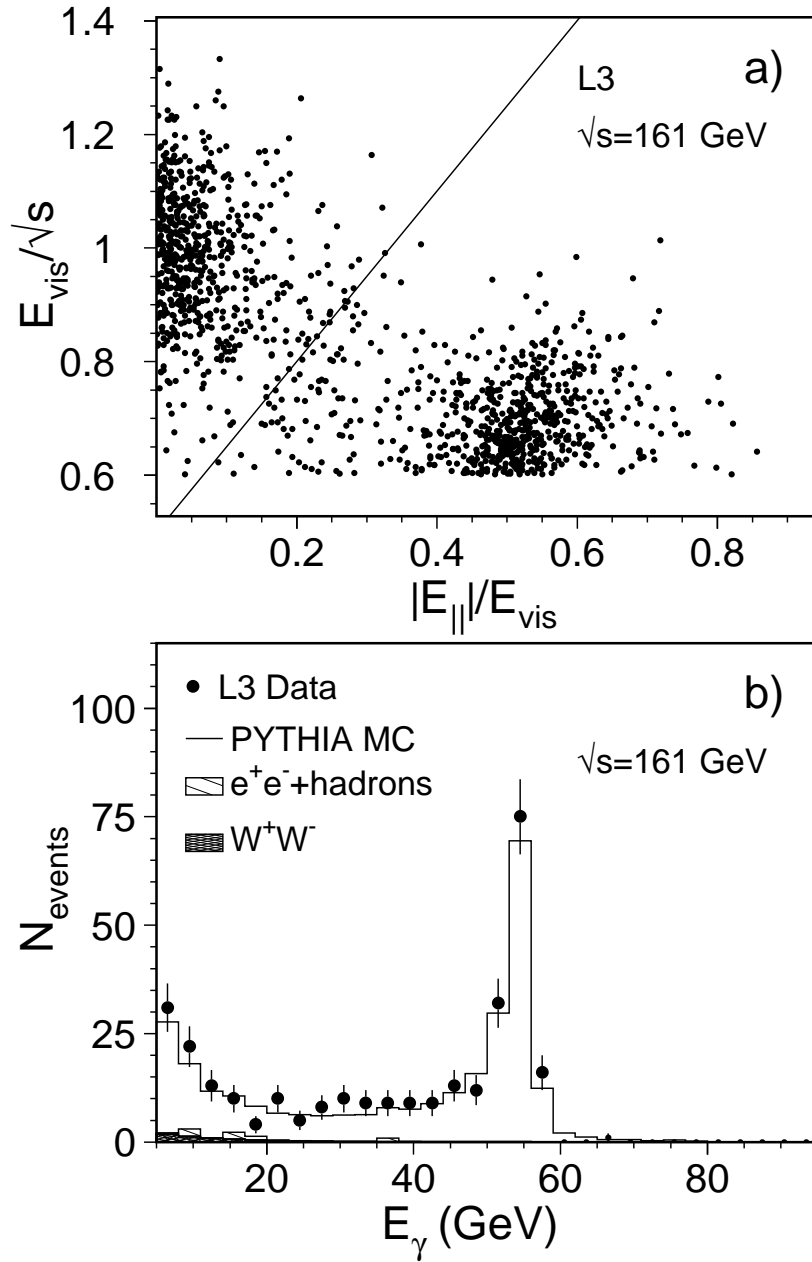


Figure 1: (a) Normalised visible energy shown as a function of the longitudinal imbalance for events at  $\sqrt{s} = 161$  GeV. The well balanced events are clearly separated from the events with hard unobserved initial state radiation. (b) Energy distribution of the most energetic photon seen in the BGO electromagnetic calorimeter.



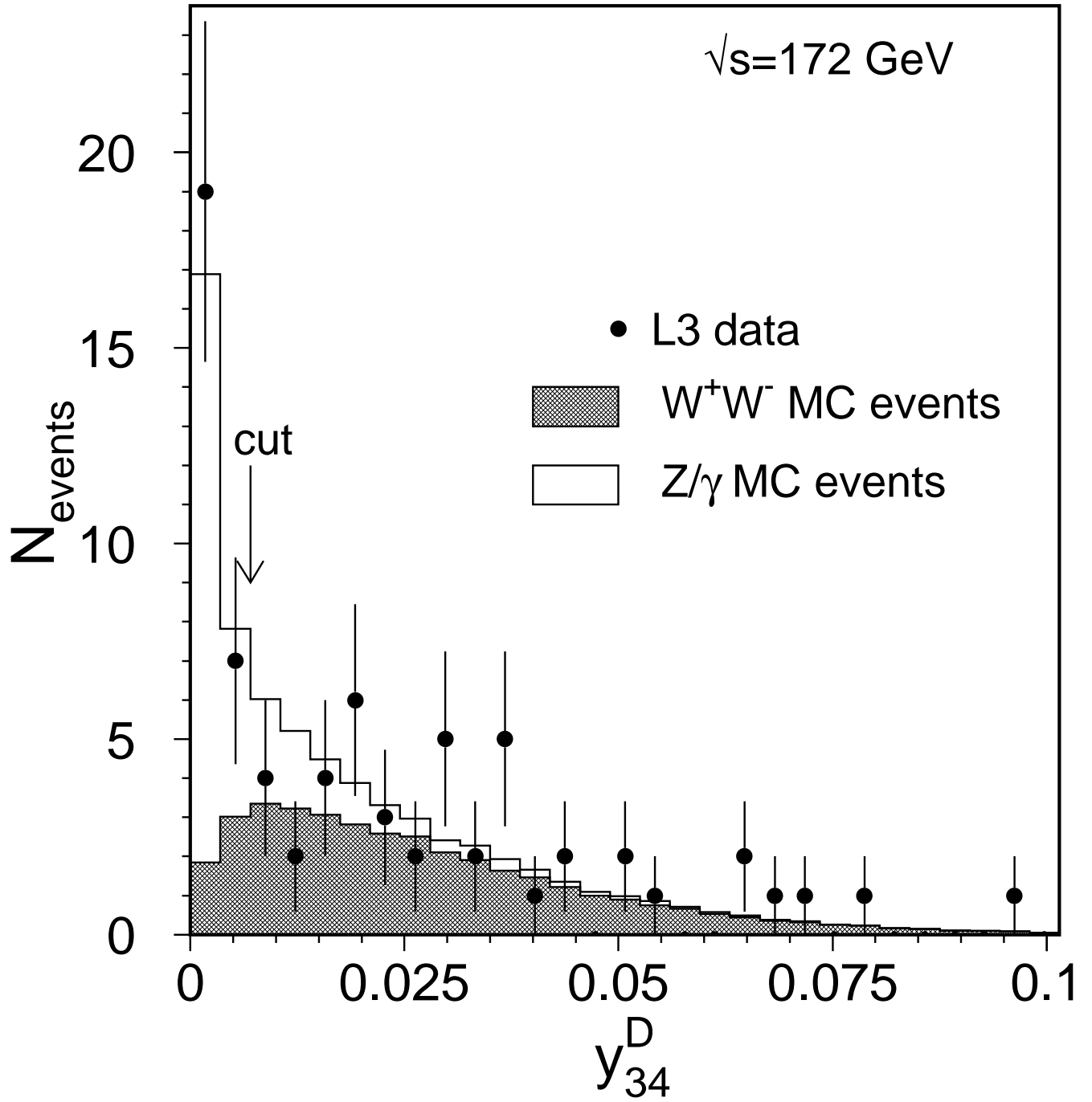


Figure 2: Distribution of  $y_{34}^D$  for events identified as  $W^+W^-$  events at  $\sqrt{s} = 172 \text{ GeV}$ .

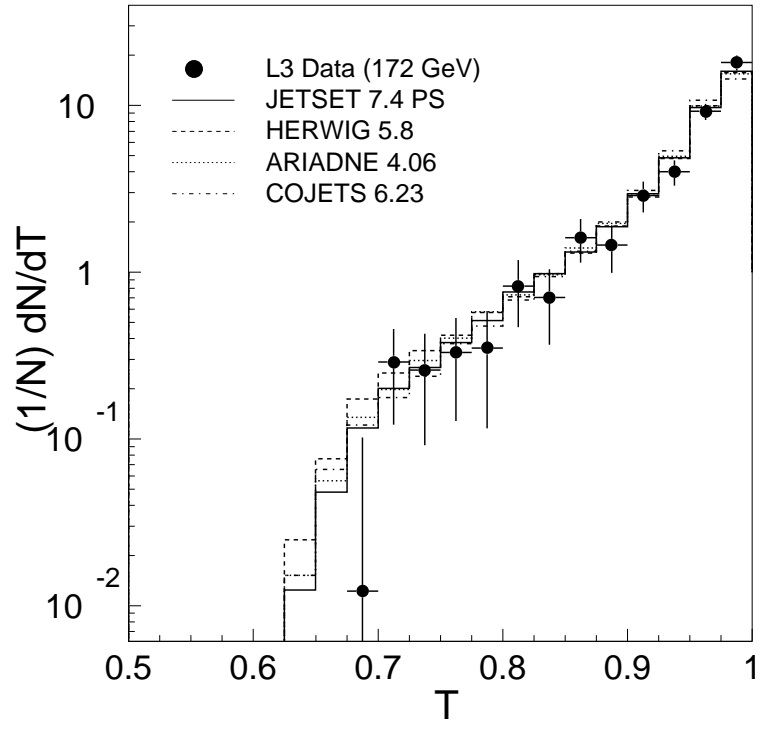
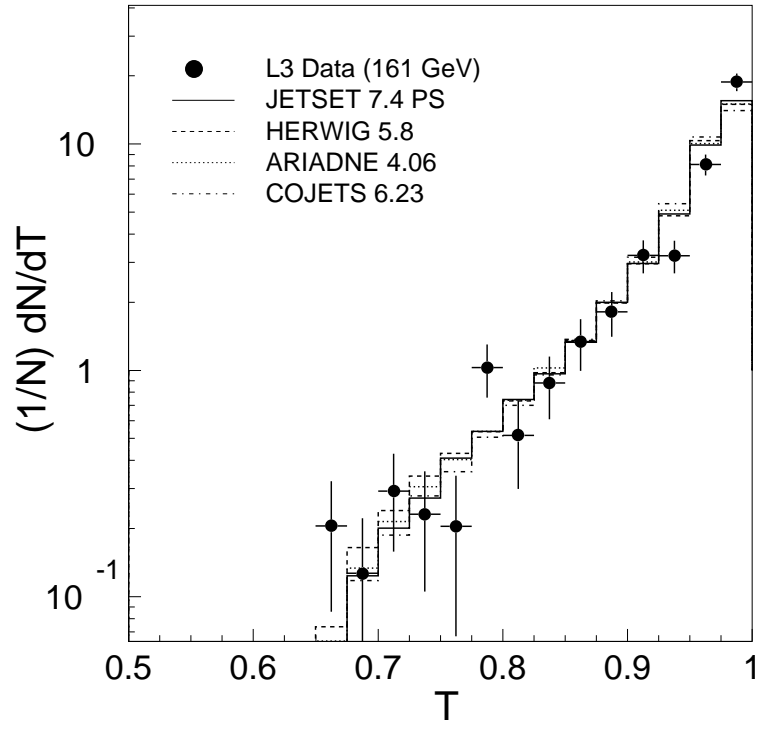


Figure 3: Corrected distributions of thrust,  $T$  at  $\sqrt{s} = 161$  GeV and 172 GeV in comparison with QCD model predictions. The experimental errors are statistical only.

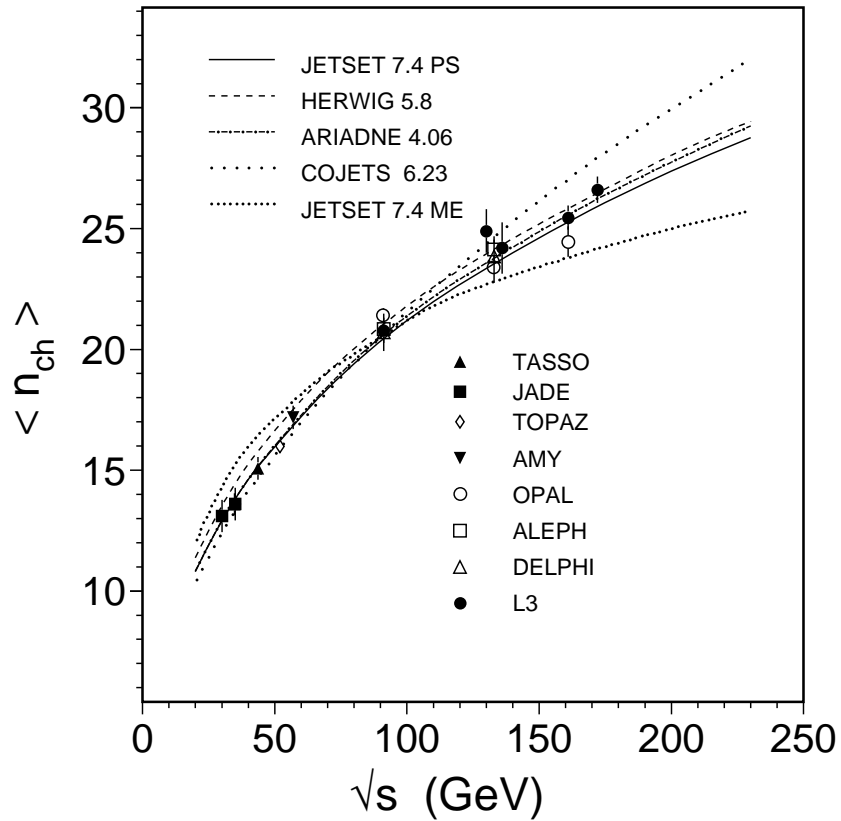
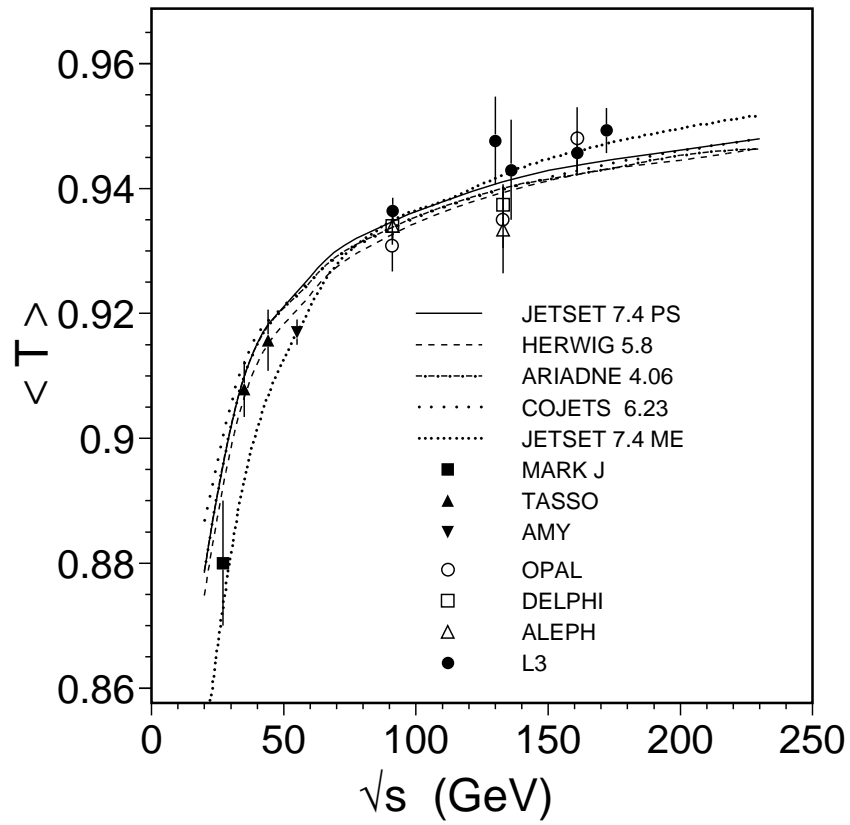


Figure 4: Distributions of mean thrust,  $\langle T \rangle$ , and mean charged particle multiplicity,  $\langle n_{ch} \rangle$ , as a function of the center of mass energy, compared to several QCD models.

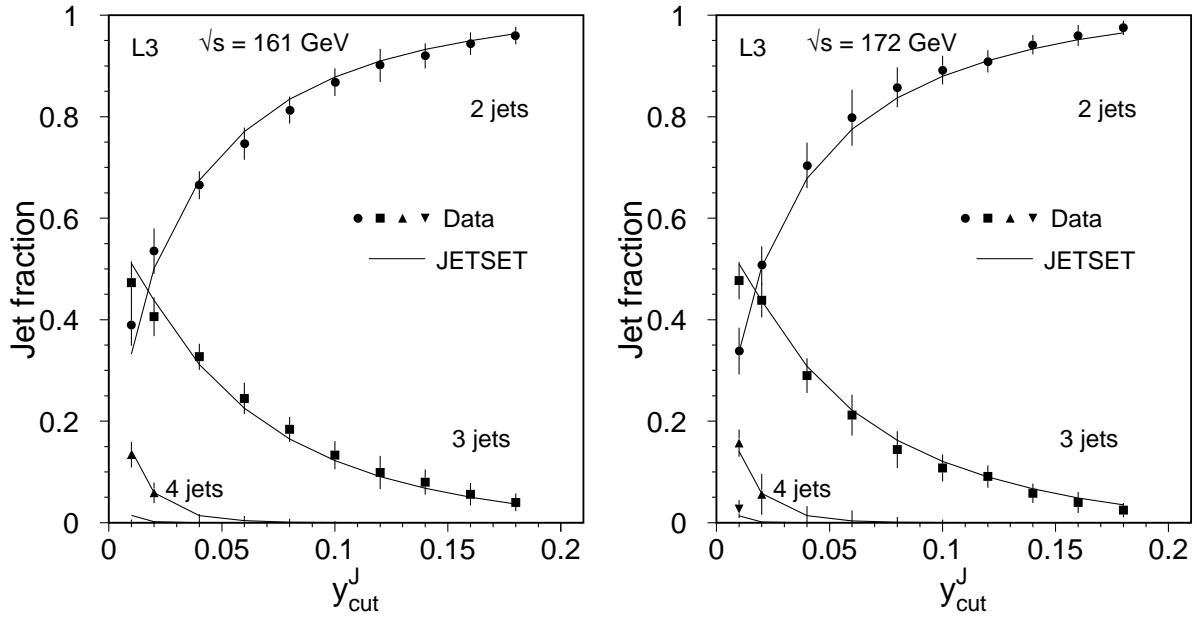


Figure 5: Jet rates as a function of  $y_{cut}$  for JADE algorithm at 161 GeV and 172 GeV. The error bars include both statistical and systematic errors added in quadrature. The lines are predictions from JETSET 7.4.

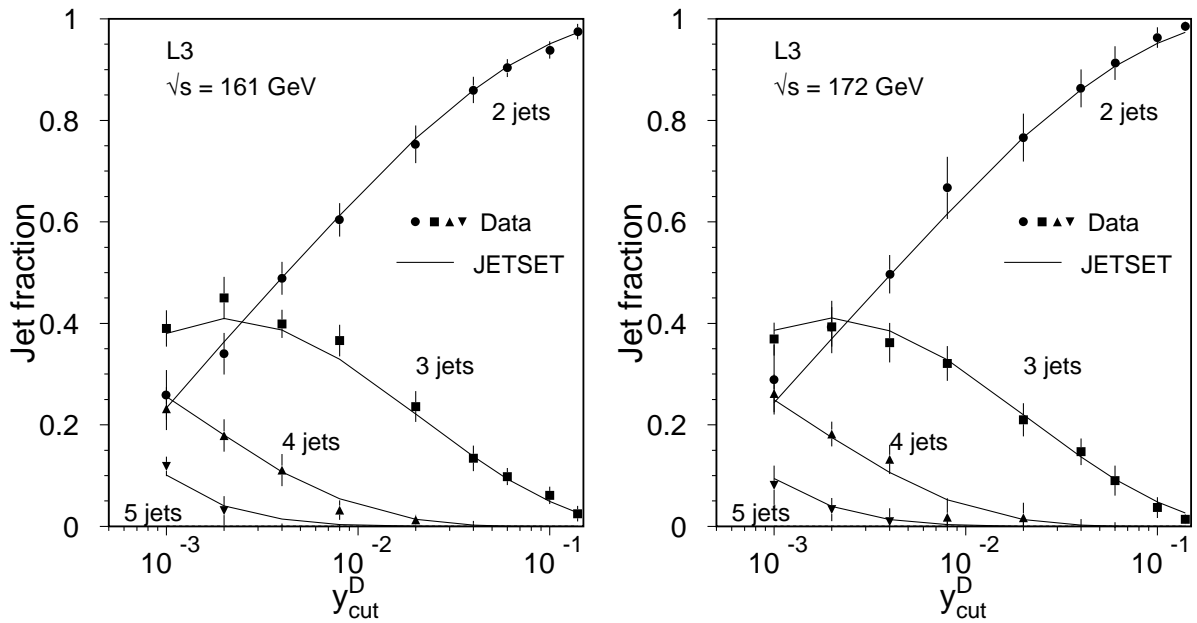


Figure 6: Jet rates as a function of  $y_{cut}$  for Durham algorithm at 161 GeV and 172 GeV. The error bars include both statistical and systematic errors added in quadrature. The lines are predictions from JETSET 7.4.

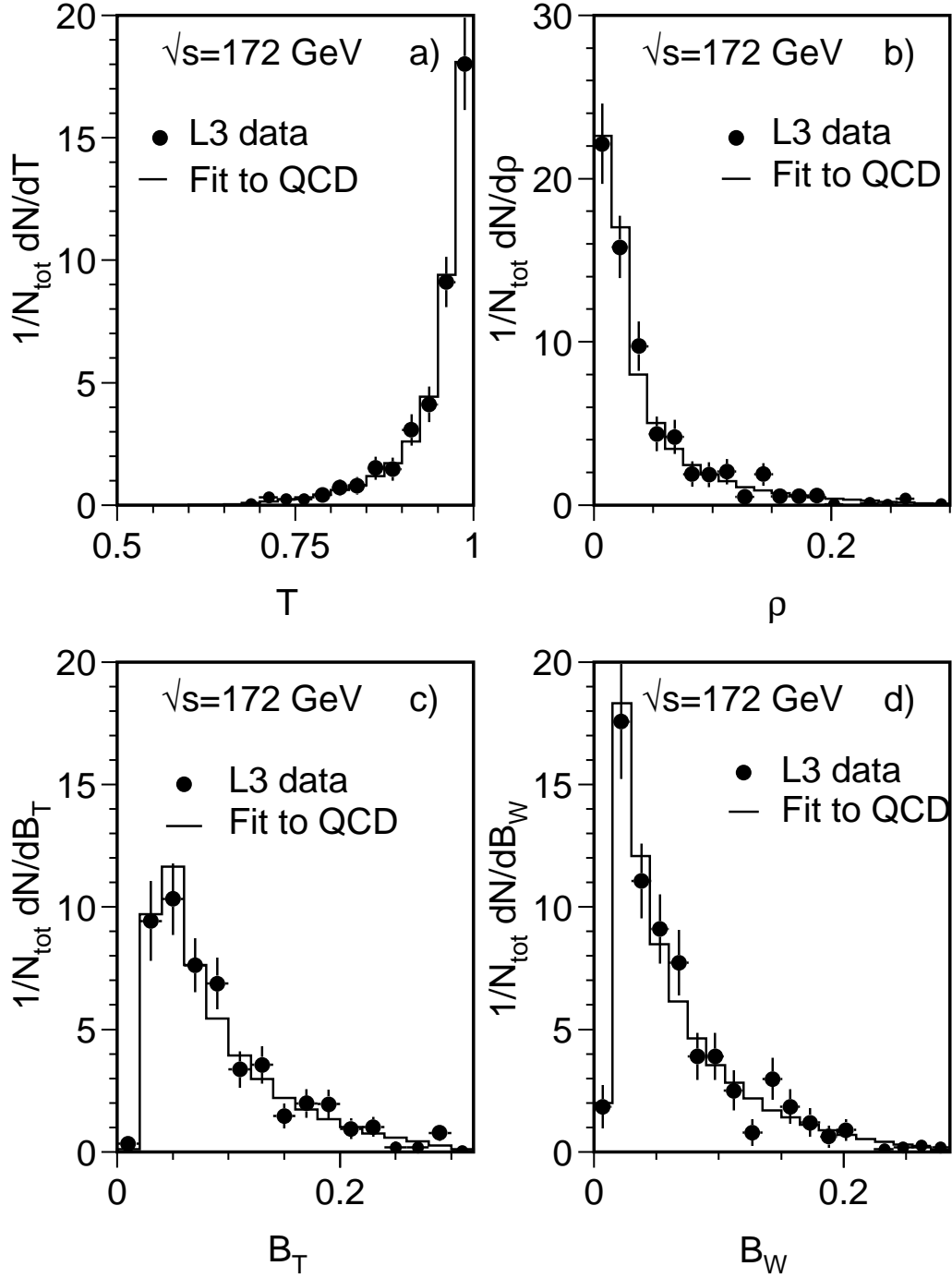


Figure 7: Measured distributions of thrust,  $T$ , scaled heavy jet mass,  $\rho$ , total,  $B_T$ , and wide,  $B_W$ , jet broadening in comparison with QCD predictions at 172 GeV. The experimental errors include statistical and systematic uncertainties.

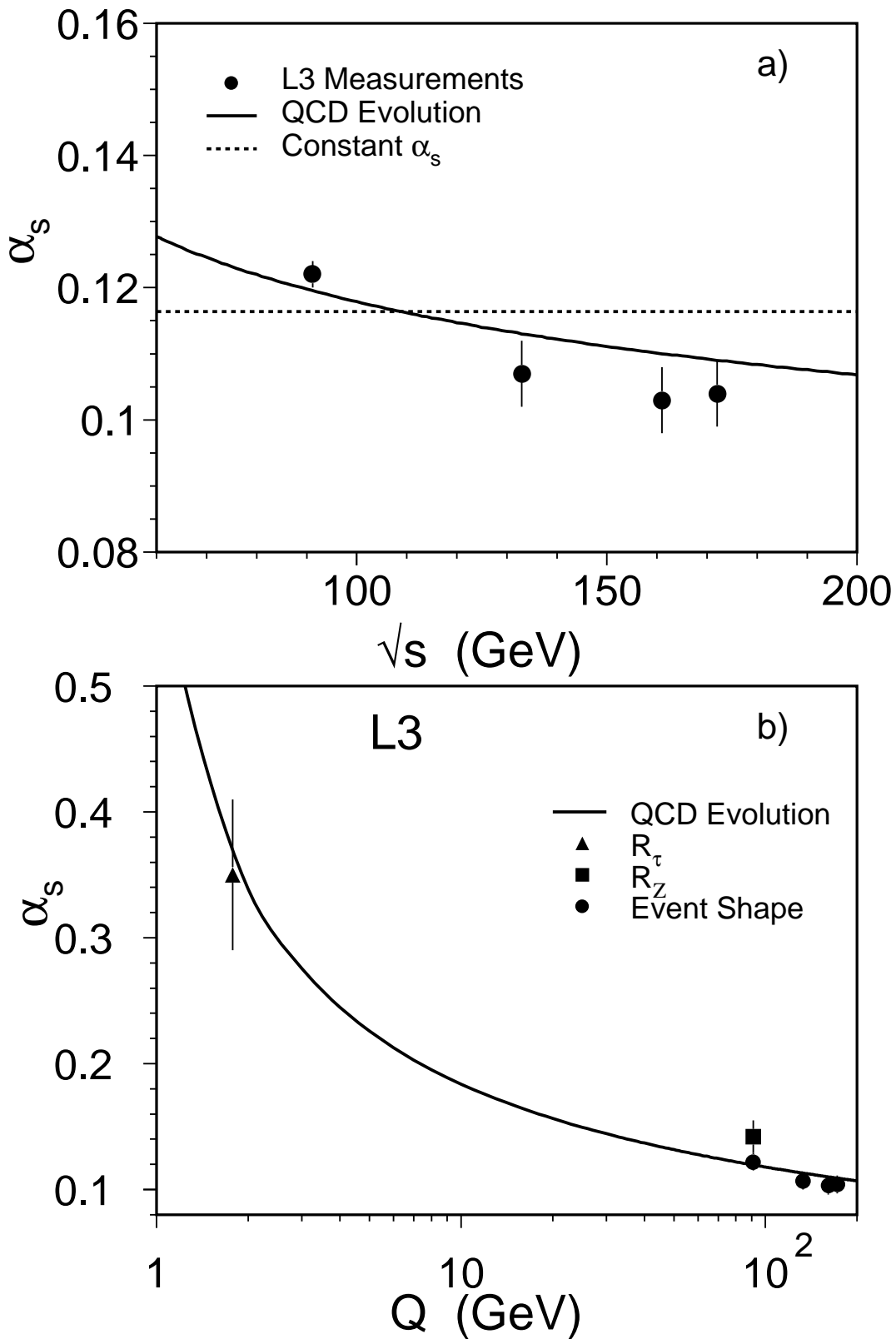


Figure 8: a)  $\alpha_s$  measurements from event shape distribution as a function of the center of mass energy. The errors correspond to experimental uncertainties. The solid and dashed lines are fits with and without energy evolution as given by QCD. b)  $\alpha_s$  values as measured by L3 from hadronic  $\tau$  decays, Z lineshape and event shape distribution. The line is a fit to the QCD evolution function to the measurements made from event shape variables.